Proceedings of the ASME 2010 3rd Joint US-European Fluids Engineering Summer Meeting and 8th International Conference on Nanochannels, Microchannels, and Minichannels
FEDSM-ICNMM2010
August 1-5, 2010, Montreal, Canada

FEDSM-ICNMM2010-30183

STATISTICAL CHARACTERISTICS IN WATER JET DISCHARGED FROM A CENTRAL-BODY NOZZLE

Can Kang
School of Energy and Power Engineering
Jiangsu University
Zhenjiang 212013,China

Feng Zhang
School of Energy and Power Engineering
Jiangsu University
Zhenjiang 212013,China

Dong Liu
School of Energy and Power Engineering
Jiangsu University
Zhenjiang 212013,China

Minguan Yang
School of Energy and Power Engineering
Jiangsu University
Zhenjiang 212013,China

ABSTRACT

As a special nozzle, central-body nozzle has attracted a lot of attention since its concept was proposed in 1980s. With Karman vortex street principle and phase-change theory, cavitation is expected to occur just after the central body. However, turbulent features in water jet flow discharged from central-body nozzle have not been illustrated by sufficient experimental data when water is ejected into ambient air. Under jet pressures of 11MPa, 13MPa and 17MPa, free water jet discharged from a central-body nozzle was experimentally studied. Phase Doppler particle anemometry (PDPA) was applied to measure non-intrusively the flow fields. Four traverse sections were selected for data visualization and representative description of the flow features. Control volumes at center and rim of the four sections were monitored for recording of every validated single droplet passing through. Experiment results indicate that pressure increase influences maximum velocity significantly. Obvious statistical characteristics exist at jet center and jet rim. The statistical feature of the droplet distribution varies slightly with pressure increase. Turbulent fluctuation is proved to be in reasonable relation to droplet behavior and droplet diameter distribution.

Key words: central-body nozzle; free water jet; statistical method; droplet diameter; control volume

INTRODUCTION

With a central body placed at nozzle center, a central-body nozzle was proposed to produce cavitation just when the fluid flows around the central body[1]. However, when water is ejected towards ambient air, reachable distance of cavitation effect is hard to be determined. If the jet pressure is elevated to be larger than 10MPa, flow characteristics will be different too.

Both theoritcal and experimental investigations of common round jet have been reported. With rapid development of computational fluid dynamics(CFD) technology, several complicated problems such as shear layer and jet stability have been tentatively studied with advanced CFD methods[2]. Even the mechanism of turbulent coherent structures of different scales are expected to be unveiled with CFD technology. However, for numerical simulation of high-pressure water jet, there are several factors that need to be comprehensively considered. Detailed problems such as droplet breakup, droplet evaporation and interaction among droplets, are difficult to be resonalbly handled with current CFD technology. Application of CFD technology in high-pressure water jet faces a great challenge[3].

Nozzle structure and jet pressure are two decisive factors for jet flow features. Obvious discrepancy can be found between

low-pressure and high-pressure water jets, and can be clearly explained by some flow features such as magnitude and distribution of kinematic energy, energy dissipation and flow pattern[4]. Difficulty in flow measurement and visualiztion under high jet pressure is evident and quantitative studies are rarely reported.

Droplet is the energy carrier and deep study of droplet's behavior is very meaningful. In a water jet, diameter distribution of liquid droplets with various sizes can be exactly obtained by using current measurement technology[5]. Critical turbulent parameters such as root-mean-square (RMS) velocity and Reynolds stress can also be acquired[6]. Even the time interval between two droplets passing through the same control volume can be measured and corresponding probability density function can be built [7].

Free Flow field discharged from a central-body nozzle is experimentally studied here with pure water at constant temperature of 20℃ being used as the medium. Jet pressures of 11MPa, 13MPa and 17MPa are set through adjusting of flow rate in the circuit. Non-intrusive measurement technique of Phase Doppler particle anemometry(PDPA) is adopted to measure flow parameters including mean velocity at certain control volume, root mean square (RMS) velocity and droplet's diameter. Relation between the nozzle structure and flow features is expected to be established through the study. And with transient sampling of PDPA, characteristics of those single droplets are to be statistically described as well.

NOMENCLATURE

D = diameter of single droplet(μm)
N = droplet amount in a sampling group
p = jet pressure (MPa)
u = axial mean velocity (m/s)
v = radial mean velocity (m/s)
d_{mean} = mean diameter(μm)
u_{max} = maximum axial mean velocity (m/s)
u_{rms} = axial root mean square velocity (m/s)
v_{rms} = radial root mean square velocity (m/s)

CENTRAL-BODY NOZZLE

The concept of central-body nozzle comes from studies in 1980s when high-pressure water jet technology was tentatively applied in some special occasions such as petroleum exploring and underground mining. According to Karman vortex street principle in fluid dynamics, when fluid flows around a blunt body, alternating wake vortices will emerge after the blunt body. Therefore, possible cavitation led by the low static pressure in vortex center or stagnation zone will appear and reinforce the action exerted on the processed object due to collapsing of cavitation bubbles near the object's surface. Concept of central-body nozzle is shown in Fig.1. Being placed at the middle of a round nozzle, a cylinder with its center axis coaxial with the symmetrical line of the nozzle is deemed as a central body. An annular space between the central body and inner wall of the nozzle is formed and fluid passes through the annular space with large velocity magnitude. In Fig.1, the two-dimensional flow feature is represented by anticipated velocity vector distribution. It can be concluded that just near the cylinder's afterbody, a stagnation zone exists with its outer fluid being consistently exposed to strong shear effect due to the difference of velocity magnitude between the jet and the stagnating fluid. Cavitation is possible to happen, but the attainable cavitating distance along the jet is considerably short for the rapid reconstruction of flow field after the jet center is filled with fluid.

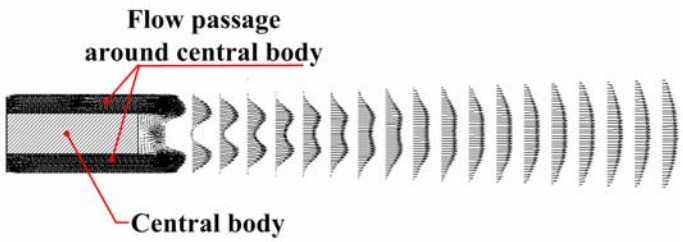

Fig.1 Jet flow discharged from a central-body nozzle

EXPERIMENTATION

As a non-intrusive measurement technology, PDPA has been widely recognized in flow velocity and droplet size measurement. According to light-wave Doppler effect in Einstein' s special theory of relativity, when an object scatters lights, consequent Doppler frequency shift is in relation to travelling speed of the object. Droplet diameter can be deduced from measured signal phase difference [8]. As far as velocity measurement is concerned, basic principle of PDPA is identical with that of laser Doppler velocimetry(LDV). Simultaneous recording of droplet diameter and droplet velocity can be achieved with PDPA. However, according to current development level of PDPA, three-dimensional synchronous measurement is difficult to be accurately realized [9].

In this study, a PDPA system produced by Dantec corporation is applied. The system is composed of an argon ion laser generator with maximum power of 5W, a two-dimensional emission probe, a receiving probe, a fiber driver, a photoelectric receiver, a data processor, control software, a three-dimensional coordinates frame and a displacement framework. For the scattering model of refraction used, a scattering angle of 35° is set in the experiment. Major parameters employed are listed in Table 1.

Table 1. Parameters of the PDPA system

Parameter	Value
Focal length	500 nm
Wavelength	514.5 nm (green laser)
	488.0 nm (blue laser)
Beam spacing	38 mm
Beam diameter	1.35 mm
Fringe spacing	6.775 μm (green laser)
	6.426 μm (blue laser)
Probe volume	0.243 mm×0.243 mm×6.389 mm (green laser)
	0.230 mm×0.230 mm×6.060 mm (blue laser)

Four sampling sections are selected along the jet direction. Axial and radial mean velocities, root-mean-square velocities and Sauter mean diameter (SMD) distributions are measured. The location of the ellipsoidal control volume is oriented through auto-adjustment of the three-dimensional coordinates frame accurately controlled by a computer. Sampling droplet amount is set to be 2000 in each complete sampling process.

A triple-cylinder plunger pump with rated power of 9kW is applied as the pressure-enhancing equipment. The pressure at the pump outlet is 23MPa. Energy losses along the high-pressure tube are taken into account. Diameter of the central body is 1mm and outlet diameter of the central-body nozzle is 1.5mm. Characteristic Reynolds number(Re) is 1.38×10^5. Since the medium is tap water, no tracer particles are needed. Schematic view of the experiment system is shown in Fig.2 and the jet flow in the experiment is displayed in Fig.3.

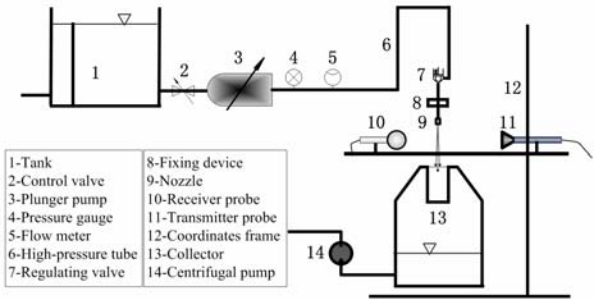

Fig.2 Sketch of the experiment system

Fig.3 Sampling with PDPA

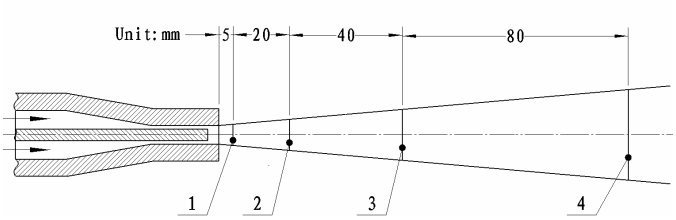

Fig.4 Sections along jet direction

Fig.4 shows the positions of the four sampling sections where PDPA data will be further analyzed and discussed. The distance between nozzle outlet and the farthest section is 145mm. Origin of coordinates of a rectangular coordinate system is set at the symmetrical center of nozzle outlet. Y-coordinates is set to be vertical to the jet flow direction.

EXPERIMENT RESULTS AND DISCUSSION

Velocity distribution

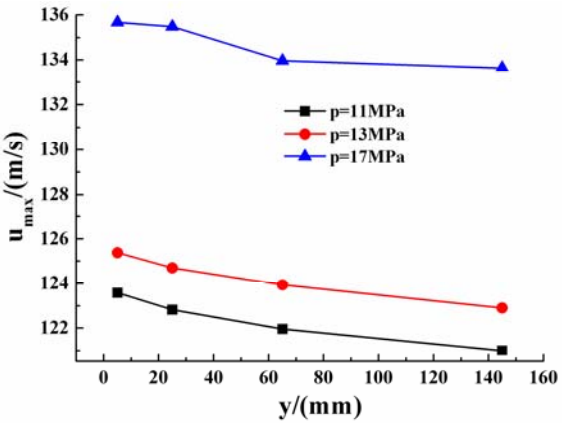

Fig.5 Dissipation of maximum velocity

Maximum velocity distribution along the jet direction is displayed in Fig.5. The variation curves are similar under different jet pressures. If a dissipation rate λ could be defined by

$$\lambda = \frac{u^1_{max} - u^4_{max}}{u^1_{max}} \quad (1)$$

Where u^1_{max} and u^4_{max} denote maximum axial velocity at Section 1 and Section 4 respectively. Under jet pressures of 11MPa and 13MPa, the nearly equivalent dissipation rate λ of maximum axial velocity is about 2.0%. When the jet pressure reaches 17MPa, dissipation rate λ of maximum axial velocity is about 1.5%. Energy-remaining ability is improved with increased jet pressure.

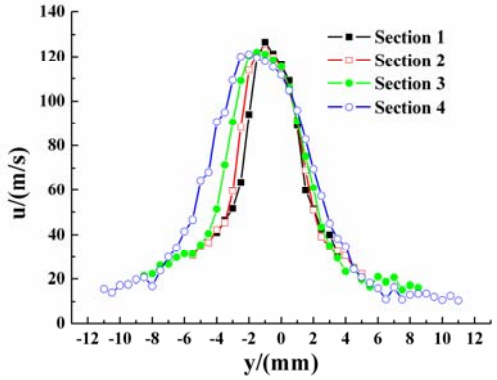

Fig.6 Axial velocity distribution at p=11MPa

Under the three jet pressures studied, similarity is considered to exist among the three corresponding jet flows, so only velocity distributions under jet pressure of 11MPa are selected for explanation of energy distribution in this kind of jet. Axial velocity distribution at jet pressure of 11MPa is shown in Fig.6, for all the four sections, distributions of axial velocity are expressed in a dimensional way, which is to illustrate the velocity magnitude under such a jet pressure level and to avoid the possible deviation due to uncertainty in determining jet width at each section. Nearly symmetrical distribution about the jet axis is found in Fig.6. Approaching the nozzle, at Section 1, the whole jet is concentrated around the jet axis and relative width of high-velocity zone is the biggest. The four sections all show different levels of axial velocity dissipation near jet rim.

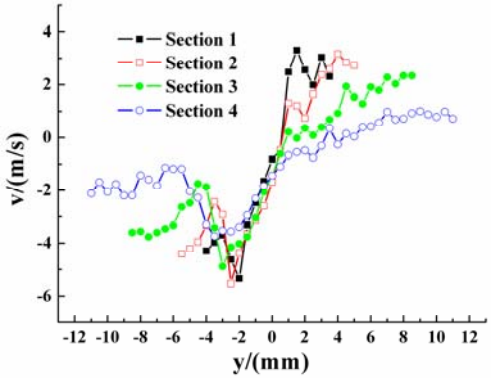

Fig.7 Radial velocity distribution at p=11MPa

Radial velocity distribution under jet pressure of 11MPa is shown in Fig.7. Four distribution curves accumulate symmetrically on both sides of the jet axis with different abscissa ranges. Near the jet rim, peak value of radial velocity appears at each section with different magnitudes. Jet concentration gets weak near the jet rim and traveling direction of droplets is greatly deflected. The traverse diffusion of the jet is proved to arouse intense interaction between water jet and ambient air and subsequent entrainment phenomenon.

RMS velocity distribution

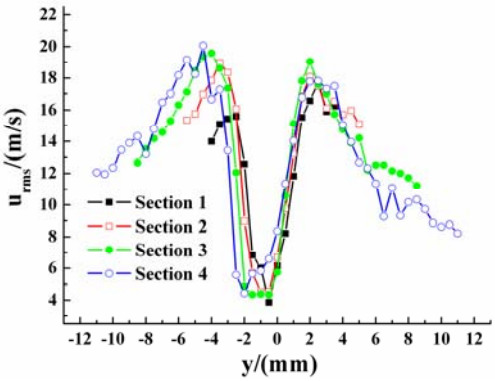

Fig.8 Axial RMS velocity distribution at p=11MPa

To study droplet behavior in the highly turbulent flow, axial RMS velocity is displayed in Fig.8. Axial RMS velocity distribution is more irregular in comparison with mean axial velocity distribution. At each section, there is a valley value of axial RMS velocity just at the jet center. The four curves mingle together except that the evident difference of traverse distance appears along the jet direction. At section 4, the discrepancy of the two extreme u_{rms} value reaches as high as 16m/s. There is an apparent highly turbulent zone symmetrically located at the two sides of jet axis.

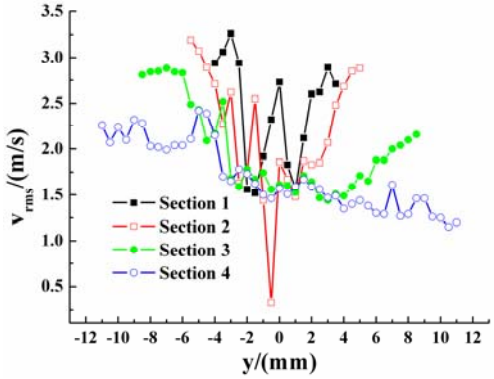

Fig.9 Radial RMS velocity distribution at p=11MPa

Radial velocity fluctuation is expressed in Fig.9. And the overall fluctuation level is lower than that in Fig.8. The restriction imposed on radial movement of droplets is greatly lightened. From Section 1 to Section 3, distributions of radial RMS velocity are totally random, especially near the jet center. At Section 4, the distribution is relatively smooth with slight difference of radial RMS velocity along the traverse direction. It should be noticed that random distribution of radial velocity near nozzle outlet is in direct relation to the intense interaction occurring at jet center.

Droplet diameter distribution

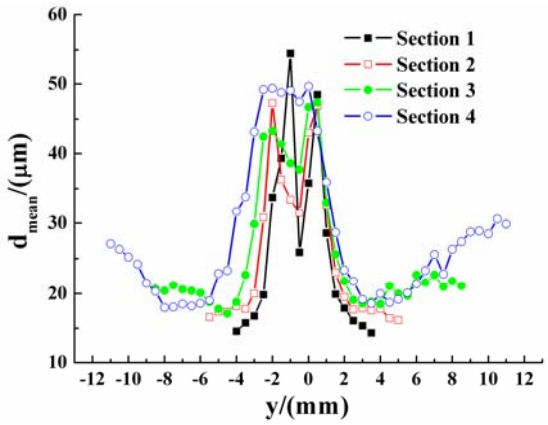

Fig.10 Droplet diameter distribution at p=11MPa

As an important parameter, mean diameter is the ensemble number mean diameter of the validated PDPA samples and is defined by:

$$d_{mean} = \frac{1}{N}\sum_{i=1}^{N} n_i D_i \qquad (2)$$

Fig.10 shows the d_{mean} distribution along the jet direction. As a whole, droplets with their d_{mean} ranging from 13-55 μm occupy the vast majority. Near the jet axis there is a valley value of d_{mean} and the valley value increases consistently from Section 1 to Section 4. Near each section's rim, there is also a valley value of d_{mean} larger than that near jet axis. At jet center, interaction led by original annular jet will drive large droplets to breakup into smaller ones. However, the size and amount of the droplets produced are greatly non-uniform. Significant fluctuation of d_{mean} near the jet axis is caused by transient variation of droplet amount within a small abscissa range.

Statistical feature

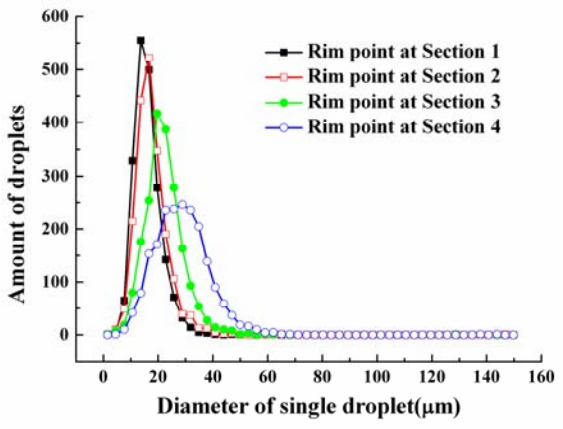

(a) p=11MPa

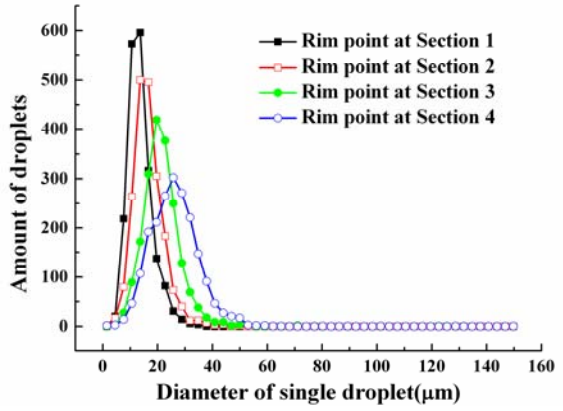

(b) p=13MPa

Fig.11 Statistical relation between droplet amount and droplet diameter at rim points

Being a decisive factor during jet energy transferring, droplet's behavior plays an important role in practical operation of the central-body nozzle. During PDPA sampling, detailed information including size, velocity and transit time of every single droplet is recorded. It is then possible to analyze the statistical features in a certain control volume. Statistical relations between droplet amount and droplet diameter at rim points under jet pressures of 11MPa and 13MPa are shown in Fig.11. With different jet pressures, the relations are uniform

for corresponding section. From Section 1 to Section 4, smaller droplets tend to possess a continually increased percentage in the sampling group. The discrepancy of amounts of droplets with different sizes becomes larger from Section 1 to Section 4.

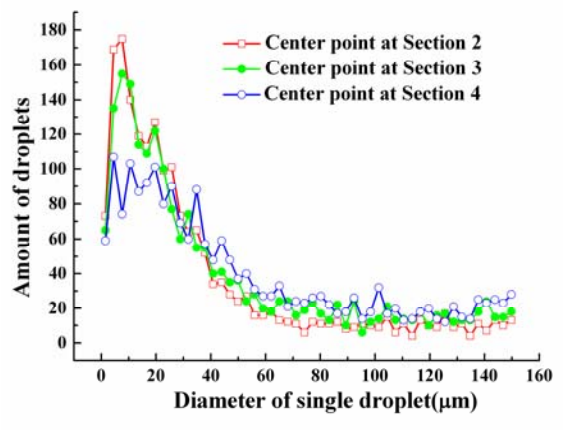

Fig.12 Statistical relation for center points

To comparatively analyze the droplet behavior at jet rim and jet center, statistical relation between droplet amount and droplet diameter is presented in Fig.12. Since the statistical distribution curves at the two center points of Section 1 and Section 2 are almost overlapping, only three curves representing center points at Section 2, 3 and 4 under jet pressure of 11MPa are displayed. The distribution of droplets with different sizes is relatively uniform compared with that in Fig.11. Droplets with their diameters less than 40μm possess the vast majority, but the corresponding amount decreases apparently. At the jet center of Section 4, the most uniform distribution is found. With the distance from nozzle outlet increased, jet energy gets dissipated and droplets at jet center are consistently produced from both shear effect between circular layers with different velocity magnitudes and the disturbance aroused by entrained air.

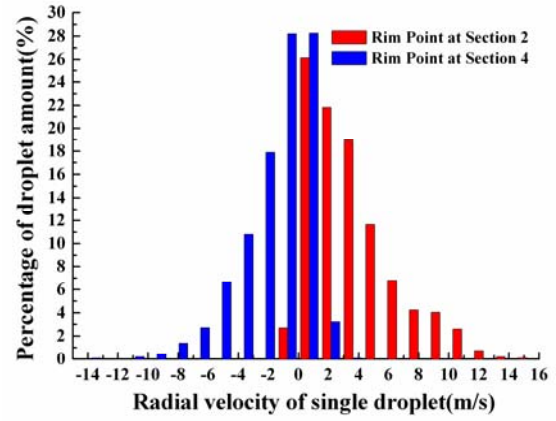

(a) p=11MPa

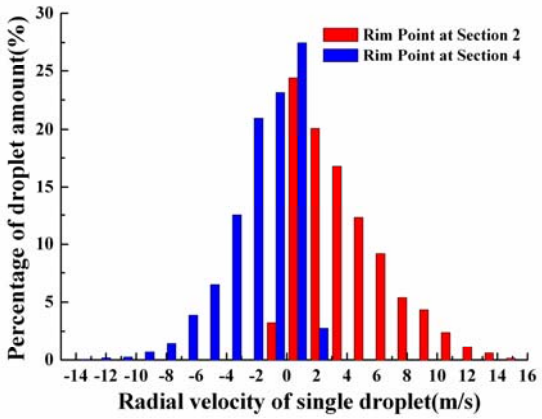

(b) p=13MPa

Fig.13 Statistical relation between percentage of droplet amount and radial velocity at rim points

To deeply analyze the droplet breakup behavior, statistical data about the radial velocity of single droplet passing through the control volume located at rim points of Section 2 and Section 4 under jet pressures of 11MPa and 13MPa are displayed in Fig.13. In view of the radial velocity distribution in Fig.7, it can be found that mean velocity at rim point is relatively large. In Fig.13, it can be well explained that contribution to large radial velocity mainly comes from the behavior of a small number of droplets. There is slight difference between the distributions in Fig.13(a) and Fig.13(b). For the same control volume, amount of droplets with high radial velocity tends to increase when jet pressure gets larger.

CONCLUSIONS

For water jet discharging from a central-body nozzle, jet pressure has positive influences on jet velocity and energy-remaining ability. Under jet pressure of 17MPa, relative energy dissipation rate can be as low as 1.5%.

Axial velocity distributions at different sections are similar with that in common round jet flow field, but radial velocity distribution is characterized by two peaks near the jet rim. The radial RMS velocity distributions prove that the influence of radial velocity on jet's traverse diffusion can not be neglected.

For the same control volume at jet rim, statistical relation between droplet amount and droplet diameter only varies slightly with variation of jet pressure. Another statistical relation between percentage of droplet amount and radial velocity at rim points is not obviously influenced by increase of jet pressure.

ACKNOWLEDGMENTS

This work is supported by the National Natural Science Foundation of China (Grant No.50806031).

REFERENCES

[1] David A.Summers. Consideration in the comparison of cavitating and plain water jets. Proceedings of the 2nd U.S. Water Jet Conference, May 24-26, 1983, pp:178-183.

[2] Fan Quanlin, Zhang Huiqiang, Guo Yincheng, Wang Xilin, Lin Wenyi. Large-eddy simulation of a round turbulent jet under the flow axisymmetric assumption. Journal of Combustion Science and Technology, 2001,7(4):248-251.

[3] Jiang Yong,Liao Guanxuan,Wang Qingan, FanWeicheng. Study on calculating model of droplets collision/coalescence in spray process. Fire Safety Science, 2000, 9(2): 27-30.

[4] MC. Butler Ellis, CR Tuck and P.C.H. MillerThe effect of some adjuvants on sprays produced by agricultural flat fan nozzles. Crop Protection, 1997 , 16(1): 41-50.

[5] G.E.Mccreery,C.M.Stoots. Drop formation mechanisms and size distributions for spray plate nozzles. International Journal of Multiphase Flow, 1996,22(3):431-452.

[6] M.Iguchi, K.Okita, F.Yamamoto. Mean velocity and turbulence characteristics of water flow in the bubble dispersion region induced by plunging water jet. International Journal of Multiphase Flow, 1998,24(4):523-537.

[7] C. Martínez-Bazán, J.L. Montañés, J.C. Lasheras. Statistical description of the bubble cloud resulting from the injection of air into a turbulent water jet. International Journal of Multiphase Flow, 2002,28: 597-615.

[8] Shen Xiong , Wei Nailong , Peng Tao. Measurement of velocity and size characteristics of water spray droplets with a laser phase doppler system. Experiments and Measurements in Fluid Mechanics. 2000, 14(2): 54-60.

[9] Xia Zhenyan, J iang Nan. The measurement on the turbulence jet with 3D LDV system. Experiments and Measurements in Fluid Mechanics, 2002,16(2):72-77.